PHILOSOPHICAL TRANSACTIONS OF THE ROYAL SOCIETY A

Phil. Trans. R. Soc. A (2009) **367**, 665–682
doi:10.1098/rsta.2008.0243
Published online 20 November 2008

Review

The coupling of winds, aerosols and chemistry in Titan's atmosphere

By Sebastien Lebonnois[1,*], Pascal Rannou[2,3] and Frederic Hourdin[1]

[1]*Laboratoire de Meteorologie Dynamique, IPSL, UPMC/CNRS, 4 place Jussieu, Box 99, 75252 Paris Cedex 05, France*
[2]*Groupe de Spectrométrie Moléculaire et Atmosphérique, Université Reims Champagne-Ardenne, Moulin de la Housse, BP 1039, 51687 Reims, France*
[3]*Service d'Aéronomie, IPSL, CNRS, BP3, 91371 Verrières le Buisson, France*

The atmosphere of Titan is a complex system, where thermal structure, radiative transfer, dynamics, microphysics and photochemistry are strongly coupled together. The global climate model developed over the past 15 years at the Pierre-Simon Laplace Institute has been exploring these different couplings, and has demonstrated how they can help to interpret the observed atmospheric structure of Titan's lower atmosphere (mainly in the stratosphere and troposphere). This review discusses these interactions, and our current understanding of their role in the context of this model, but also of other available works. The recent Cassini results, and the importance of the production mechanisms for Titan's haze, have put forward the need to explore the mesosphere and the couplings between upper and lower atmosphere, as well as the current limits of available models.

Keywords: Titan; atmosphere; dynamics; aerosols; composition

1. Introduction

The Voyager spacecraft visits to Saturn's system in the 1980s had revealed that Titan, its largest satellite, had a complex atmospheric system. Its surface is hidden behind a veil of hydrocarbon haze, a by-product of the complex photochemistry induced in the upper atmosphere by the photodissociation of methane, its most abundant atmospheric compound (approx. 1.5%) except for nitrogen (approx. 98%). From the analysis of these sets of observations, it became clear in the early 1990s that dynamics, haze and clouds microphysics and photochemistry cannot be studied separately in Titan's atmosphere (Toon *et al.* 1992; Bézard *et al.* 1995; Hutzell *et al.* 1996). To understand this system, sophisticated climate models had to be developed, including couplings between

* Author for correspondence (sllmd@lmd.jussieu.fr).

One contribution of 14 to a Discussion Meeting Issue 'Progress in understanding Titan's atmosphere and space environment'.

atmospheric dynamics, radiative transfer, microphysics and photochemistry and their spatial and temporal variations. Similar models have already been developed for the Earth's atmosphere during the last few decades, and are also well advanced for Mars' climate studies.

The Cassini–Huygens mission now enables a detailed analysis of Titan's atmosphere and surface, sending abundant data that will help to answer many questions, and will ask many others: how do these coupled systems currently behave? How did they behave in the past? What is their history, and what does it tell us about the Solar System's and the Earth's history? To address these questions, it became essential to use global climate models similar to those developed for the Earth in the last few decades to address many concerns about our own climate (including its evolution under the effects of human activity).

Fifteen years ago, the three-dimensional global climate model of Laboratoire de Météorologie Dynamique, within the Pierre-Simon Laplace Institute, was adapted to Titan. The first version covered the troposphere and stratosphere, from the surface up to 250 km altitude, without couplings with haze or composition. It predicted a strong superrotation of Titan's atmosphere, with stratospheric winds of the order of $100\,\mathrm{m\,s^{-1}}$, approximately 10 times the equatorial rotation speed of Titan (Hourdin *et al.* 1995). This model gave the first global view of Titan's atmospheric dynamics, including spatial and seasonal variations. In parallel, a microphysical model of Titan's haze layers was elaborated at Service d'Aéronomie (Cabane *et al.* 1992; Rannou *et al.* 1995), and a photochemical model was developed at Centre d'Etude Spatiale des Rayonnements, in Toulouse (Lebonnois 2000; Lebonnois *et al.* 2001). The full coupling of these tools within the general circulation model (GCM) was completed 5 years ago (Hourdin *et al.* 2004; Rannou *et al.* 2005), and the upper limit has been extended to roughly 500 km, just above the top of the modelled haze layer.

The coupled calculations of haze microphysics, radiative transfer, photochemistry and circulation have only been possible in two dimensions (latitude–altitude) until now, due to computation costs. In this axisymmetric model (with respect to polar axis), variations in longitude are not explicitly accounted for. Non-axisymmetric processes, mainly barotropic waves that mix momentum, haze and chemical trace species, have been parametrized based on three-dimensional simulations (Luz & Hourdin 2003; Luz *et al.* 2003).

In this review, we show that despite its current limitations, this GCM has been successful in explaining many of Titan's atmospheric characteristics, with emphasis on the role of the different couplings between circulation, aerosols and photochemistry. Section 2 presents the main features of the modelled circulation. In §3, it is shown with the model how the large-scale structures in the haze layers are driven by the meridional circulation, and how the haze structures, in return, affect thermal structure and atmospheric circulation through radiative feedback. Our results are consistent with and explain the latitudinal profiles of stratospheric composition that were obtained by the Voyager 1 spacecraft (Coustenis & Bézard 1995), and recently by CIRS onboard the Cassini spacecraft (Flasar *et al.* 2005; Coustenis *et al.* 2007). These results emphasize the role of the meridional circulation on compound distributions (§4). Modelling of tropospheric clouds is also included (Rannou *et al.* 2006), and comparisons between modelled cloud distributions and clouds observed recently in Titan's troposphere, with ground-based observations (Roe *et al.* 2002) and by Cassini instruments

(Griffith *et al.* 2005; Porco *et al.* 2005), give insight into the role of dynamics in the tropospheric methane cycle (§5). It may even help to predict the seasonal evolution of the cloud cover, as discussed in §6. In §7, we discuss the limitations of this GCM, and other processes that are not taken into account yet, but appear to play a significant role in Titan's climatic system: the effects of the Saturnian tides in the troposphere (Tokano & Neubauer 2002), the upper atmospheric chemistry, which may produce the haze precursors, and therefore couple the upper and lower regions of the atmosphere (Waite *et al.* 2005).

2. Stratospheric and tropospheric dynamics

Direct observations of the atmospheric dynamics in Titan's atmosphere are sparse. Zone winds have been measured from the Earth using stellar occultations (Hubbard *et al.* 1993; Sicardy *et al.* 2006) or using Doppler-shift measurements in millimetre (Moreno *et al.* 2005) or infrared wavelengths (Luz *et al.* 2005). They have also been measured *in situ* using the Doppler Wind Experiment onboard Huygens (Bird *et al.* 2005), and inferred from thermal structure based on CIRS/Cassini data (Flasar *et al.* 2005; Achterberg *et al.* 2008). These measurements show that the atmosphere of Titan is in superrotation, the whole atmosphere rotating faster than the solid body. To understand such a circulation regime, GCMs are very useful tools.

The main features of meridional circulation in the stratosphere inferred from our GCM's simulations are presented in figure 1, together with the zone wind. The main circulation is a large pole to pole meridional direct cell, with a broad ascending branch in the summer hemisphere and a descending branch in the winter polar region (figure 1*a*). This circulation is thermally direct, forced by solar heating. It is quite similar to the Hadley circulation in the Earth tropics, though with some differences: (i) the ascending branch follows the maximum of solar heating, and therefore moves much closer to the summer pole than on the Earth, where the surface thermal inertia maintains it close to the equator and (ii) the induced-latitudinal pressure gradient is not balanced by the Coriolis force (due to the large rotation period of Titan), but by the centrifugal force (therefore related to strong winter zone winds). This main circulation starts approximately 3 terrestrial years after the equinox and lasts until the following equinox. A full Titan year is equal to 30 terrestrial years. The period of 3 years just after equinoxes corresponds to a transition circulation where the ascending branch moves from one hemisphere to the other, lagging behind the subsolar latitude (figure 1*b*,*c*). During this transition period, a system of two cells is visible, with one ascending branch in the tropical region or near the equator, and two descending branches in polar regions. Inertial instabilities present in the equatorial region induce the alternating cells pattern seen mainly during the transition period, in the equatorial ascending branch. The spring cell retreats towards the summer pole, but does not disappear completely. A small cell, remnant of the previous season's cell, is still present in the model in the lower stratosphere (60–1 mbar), between the summer pole and the ascending motion of the dominant pole-to-pole cell (figure 1*a*,*d* for the opposite season). This ascending branch reaches from 30–40° at 60 mbar to the summer pole at roughly 1 mbar.

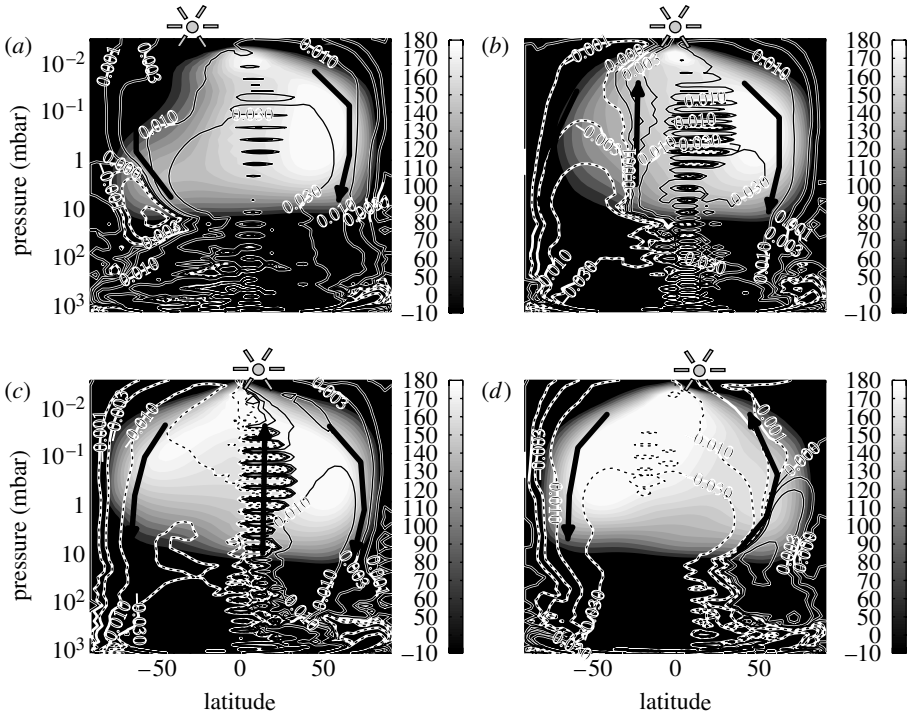

Figure 1. Zone wind ($\mathrm{m\,s^{-1}}$) and meridional stream function ($10^9\,\mathrm{kg\,s^{-1}}$, solid line is clockwise rotation, dashed line is anti-clockwise) at different solar longitude between the northern winter soltice and the end of the northern spring: (*a*) $L_s = 270°$ (northern winter soltice), (*b*) $L_s = 0°$ (northern spring equinox), (*c*) $L_s = 30°$ (in first half of northern spring), (*d*) $L_s = 60°$ (in second half of northern spring). The Sun indicates the approximate latitude of the subsolar point.

The large pole-to-pole stratospheric cell is the main circulation pattern, lasting 80 per cent of a Titan year. It is noteworthy that according to our model, Voyager and Cassini–Huygens observations occurred with such a circulation pattern. The annual mean meridional circulation, though, corresponds to the symmetric pattern with the ascending motion over the equator, and two equator-to-pole cells (similar to figure 1*c*). This may be understood, given the asymmetry of the solsticial dominant cell: subsidence appears to be more concentrated over the winter pole, while upwelling is more distributed over the overall summer hemisphere (figure 1*a*). Averaging the stream functions of both solstices thus yields ascending motions over the equator, and subsiding motions over the poles, consistent with the differential heating between equator and poles when considered on an annual basis. It must be noted that, as for other atmospheres including that of the Earth, the meridional circulation, although fundamental for the climate engine, is weak and very difficult to observe directly. The only observational confirmation of the GCM results in that respect comes from the advection of chemical compounds and haze, as discussed below.

Concerning the zone circulation, Titan's atmosphere is superrotating. The zone wind has a strong jet in the winter hemisphere located near 1 mbar. This is related to transport of angular momentum by the mean-meridional circulation: the meridional cells transport angular momentum upwards, and towards the

poles, producing acceleration of the stratospheric zone winds. The angular momentum is then redistributed towards the equator by barotropic waves, inducing equatorial superrotation. This mechanism, seen in the GCM simulations is known as the Gierasch–Rossow mechanism (Gierasch 1975; Rossow & Williams 1979). The winter jet is barotropically instable on its equator-ward flank, and in the initial three-dimensional version of the GCM, barotropic waves were developing in this region. In the two-dimensional restriction of the GCM, the mixing associated with these waves had to be parametrized (Luz & Hourdin 2003; Luz *et al.* 2003). In regions were barotropic instabilities are diagnosed, a horizontal mixing coefficient is computed, and this dissipation mimics the effects of the three-dimensional barotropic waves. The simulated meridional structure of the stratospheric zone wind is in good agreement with recent Cassini/CIRS data analysis by Achterberg *et al.* (2008). In this paper, the temperature field retrieved from CIRS spectra is used to compute zone winds through the thermal wind equation. A detailed comparison between available observations (temperature, zone wind) and the GCM simulations is presented by Crespin *et al.* (2008).

In the troposphere and lower stratosphere, the modelled circulation is much more complex (lower region of each part of figure 1). A cell system is visible with an ascending branch beyond tropics of the summer hemisphere, and descending branches at 60° of both hemispheres. Poleward of 60°, and reaching the poles, 'oblique' cells are present with ascending (descending) branches travelling through latitudes as air rises (descends) in altitude. In addition, the troposphere is a place where many instabilities are present in the model, which probably produce a strong mixing that contributes to the transport.

3. Stratospheric haze and dynamics

Haze and dynamics are coupled through a strong positive feedback loop (Rannou *et al.* 2002, 2004). The haze is initally formed in the mesosphere as small nanometric particles. This size corresponds to a threshold beyond which growth by coagulation dominates growth by chemical processes. The exact source function is not known, and strongly depends on the chemistry processes that form the macromolecules. In the GCM, the aerosol source is assumed to be uniform with latitude and in a vertically narrow zone (the formation zone) located at approximately 400 km altitude. It is not coupled to photochemistry yet, and the total flux of mass injected is a model parameter. The newly formed small particles are transported towards the winter polar region by the upper branch of the circulation. While they are transported, they also grow, reaching radii of a few tens of nanometres at the pole. Once aerosols reach the winter pole, the mean meridional circulation drives them downwards, into the stratosphere. Then, dynamical mixing time constants are short enough for the haze to be redistributed over all latitudes, although the winter descending motions maintain a strong enrichment in the winter polar regions (figure 2).

Below the formation zone, Titan aerosols grow as opened aggregates of small spheres with a fractal structure (Cabane *et al.* 1992), yielding particles that have a large effective mobility. The ratio of their mass to surface is comparable to that of the small spheres that they are made of. Even larger aerosols can thus be

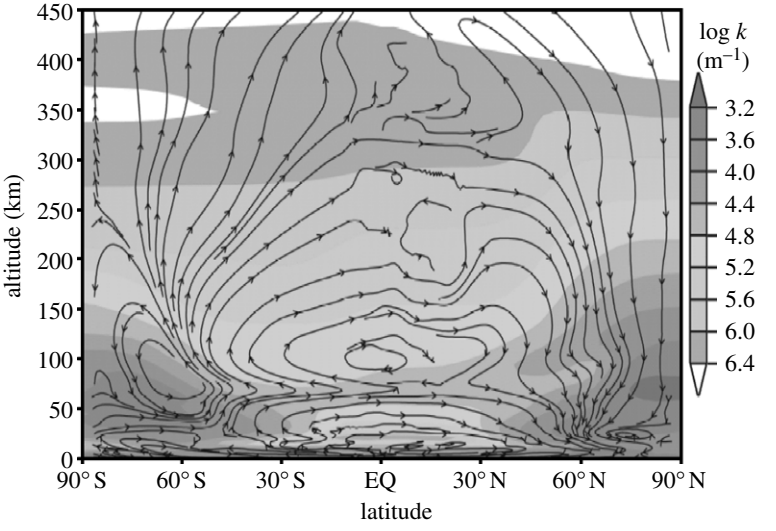

Figure 2. Meridional distribution of the haze extinction at 620 nm, 1 terrestrial year before the time of Cassini arrival. The average direction of the wind is indicated by the lines with arrows.

transported as easily as small particles of a few tens of nanometres, especially upwards. Therefore, it is noteworthy that the formation layer is also fed in large aerosols coming from lower layers, brought there by the upward circulation. Aerosols accumulate at the top of the stratospheric wind cell, which corresponds to the formation layer, and at the same time, to the detached haze layer. This is consistent with images made by the ISS/Cassini instrument (Porco *et al.* 2005). In this detached layer, because small freshly created aerosols coexist with larger coagulated aerosols, the aerosol distribution is in fact widely polydispersed, whereas the main layer has a modal aerosol distribution.

The last noticeable haze pattern is the north–south asymmetry. Its cause is to be found in the winter polar region. The stratospheric air in this region is enriched in aerosols and in chemical species (e.g. C_2H_6, C_3H_4, C_4H_2, HCN and other nitriles—see Coustenis & Bézard (1995) and Flasar *et al.* (2005)). During the descent, while the air gets cooler above the tropopause, a fraction of the aerosols are used as cloud condensation nuclei. They are then trapped and settle with the cloud drops. Therefore, air in the ascending branch of the stratospheric circulation in the summer hemisphere is found to be significantly less loaded in aerosols than air in the winter hemisphere. In the model, a sharp latitudinal variation of haze opacity is obtained close to 15° of latitude in the summer hemisphere. This induces a north–south constrast in the scattered intensity which is consistent with observations (Smith *et al.* 1982; Porco *et al.* 2005). However, detailed comparisons at different wavelengths are not fully satisfying (Rannou *et al.* 2002). The contrast between the two hemispheres is very sensitive to the structure of the atmosphere (molecules, haze, clouds and possible mist). Then, beyond the description of dominant properties, a good match between observed and modelled asymmetry intensities at several wavelengths is difficult without a very good knowledge of the scatterers' distribution in the lower atmosphere. This is not possible with the GCM.

The haze structure affects temperature and the winds. With the model, we could determine that the feedback of the haze on circulation is essentially produced by the accumulation of haze in the winter polar night, due to the circulation, as explained above. Schematically, everywhere in the stratosphere where the Sun can illuminate the haze, a local increase of haze produces an increase in diabatic heating (haze absorption) which is offset by infrared radiative cooling to space (haze emission). The only place where this does not occur is in the winter polar night, and this is also the place where the larger accumulation of haze occurs. There, the haze dramatically cools the atmosphere without the increased heating counterpart (solar radiation absorption), and then strongly increases the latitudinal contrasts of net heating rate. As a response, the mean meridional circulation is enhanced by a factor of about two, compared to a case where haze is uniformly set on the planet. This results in a larger latitudinal contrast of the temperature field, as well as an enhancement of the zone circulation (related to the increased mean meridional transport of angular momentum) which were found in better agreement with observations in the coupled model than in a model with a uniform haze (Rannou *et al.* 2004).

4. Composition and dynamics

The atmosphere of Titan is mainly composed of nitrogen (95–98%), with 1.4 per cent of methane (CH_4) in the stratosphere, and up to 5 per cent in the troposphere (Niemann *et al.* 2005). Methane and nitrogen are photodissociated in the upper atmosphere (above the mesosphere) and the obtained radicals induce a rich photochemistry, producing many hydrocarbons (e.g. C_2H_2, C_2H_4, C_2H_6, C_3H_4, C_3H_8 and C_4H_2) and nitriles (e.g. HCN, HC_3N and CH_3CN). These trace compounds are transported downwards from their production region (ranging from the upper mesosphere to the stratosphere) by atmospheric dynamics, and many of them condense in the lower stratosphere, as temperatures decrease towards the tropopause level.

The composition of Titan's stratosphere has been observed with the IRIS/Voyager 1 spectrometer, at several latitudes, and significant enrichments of several components (C_2H_2, C_2H_4, C_3H_4, C_3H_8, C_4H_2, HCN and other nitriles) were seen over the Northern Polar region. At that epoch (shortly after northern spring equinox), these latitudes were just coming out of the winter polar night period (Coustenis & Bézard 1995). It was first suggested that this unexpected enrichment may be due to accumulation of compounds in the polar night, due to seasonal inhibition of photochemical processes by lack of ultraviolet flux (Yung 1987). Lebonnois & Toublanc (1999) showed that this process was not efficient enough to explain the observed enrichment, using a three-dimensional computation of actinic fluxes (i.e. photodissociating fluxes) in Titan's atmosphere and a one-dimensional photochemical model adapted to any latitude. They suggested that this characteristic was due to meridional transport of chemical compounds.

This coupling between composition and dynamics has been studied with two-dimensional models (Dire 2000; Lebonnois 2000; Lebonnois *et al.* 2001). The model used by Dire (2000) was a GCM thermally forced by Newtonian heating: the temperature structure is relaxed towards a reference structure, with a given

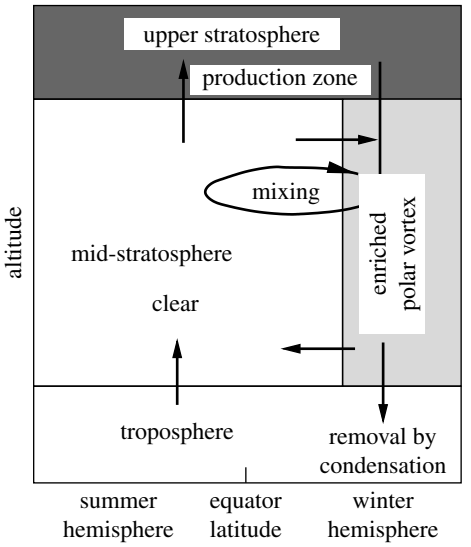

Figure 3. A sketch of the essential mechanisms responsible for the observed contrasts in Titan's stratospheric composition (adapted from Hourdin *et al.* 2004).

time constant. This GCM was coupled with a photochemical model. The altitude of the model was limited to below 250 km. Advection by meridional transport did affect the distribution of chemical compounds (C_2H_2, C_2H_6, C_3H_4 and C_3H_8), but modelled enrichments were smaller than observed. Lebonnois (2000) developed a two-dimensional photochemical model, coupled with advection by an analytic formulation of the meridional circulation, adapted to mimic the three-dimensional GCM results from Hourdin *et al.* (1995). This model included 40 chemical species, among which were all the observed hydrocarbons and nitriles. In this model, the enrichment obtained in winter polar regions was much larger, in reasonable agreement with observations. These models demonstrated that the meridional transport strongly affects the latitudinal distribution of compounds, and is able to induce the seasonal enrichments observed in the stratosphere at high latitudes at the Voyager 1 season. These processes were further analysed directly within our two-dimensional Titan GCM by Hourdin *et al.* (2004), which showed how the stratospheric contrasts are controlled by production in the upper atmosphere, condensation sink in the lower stratosphere, meridional transport and latitudinal mixing by barotropic planetary waves. These mechanisms are summarized in figure 3.

The analysis of Cassini/CIRS nadir observations has recently confirmed this stratospheric enrichment of many hydrocarbons and nitriles over the winter pole (Flasar *et al.* 2005; Teanby *et al.* 2006; Coustenis *et al.* 2007). Seasonal variations are seen between the Cassini epoch (early northern winter) and the Voyager 1 epoch (just after northern spring equinox), with enrichment of minor species that increase with the season, as Titan goes through northern winter (Coustenis *et al.* 2007; Teanby *et al.* 2008). This evolution is in agreement with the GCM, owing to ongoing downwelling in the spring polar region, well beyond the spring equinox.

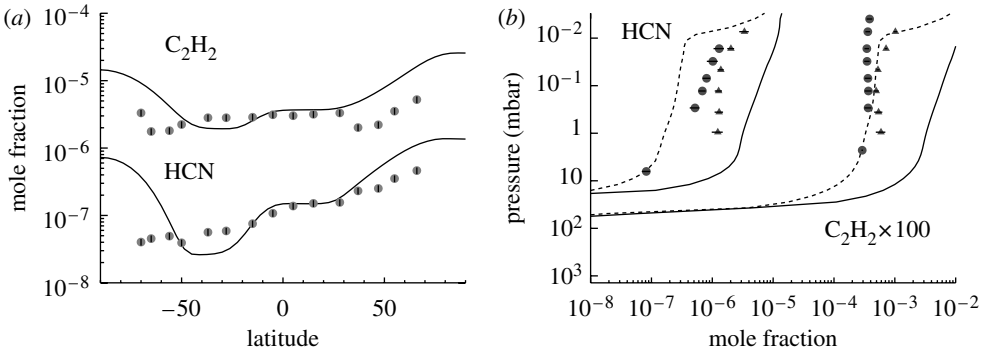

Figure 4. Mixing ratios of acetylene (C_2H_2) and hydrogen cyanide (HCN) at the Cassini epoch ($L_s \sim 300°$): (*a*) retrieved latitudinal profiles from Cassini/CIRS (circles, Coustenis *et al.* 2007) compared with GCM profiles (solid lines, Crespin *et al.* 2008) in the lower stratosphere (2–10 mbar region); (*b*) retrieved vertical profiles from Cassini/CIRS (circles for 15° S, triangles for 80° N, Vinatier *et al.* 2007), compared with GCM profiles (dashed lines for 15° S, solid lines for 80° N, Crespin *et al.* 2008). Acetylene mixing ratios have been multiplied by 100 for a clear distinction between both compounds.

Analysis of Cassini/CIRS limb observations has recently allowed one to obtain vertical profiles of several chemical compounds (C_2H_2, C_2H_4, C_2H_6, C_3H_4, C_3H_8, C_4H_2, C_6H_6, HCN and HC_3N) in the altitude range between roughly 100 and 450 km, for equatorial and high northern latitudes (Teanby *et al.* 2007; Vinatier *et al.* 2007).

Crespin *et al.* (2008) have compared in detail available observations of chemical compounds' distributions with the GCM simulations. This analysis confirms that these distributions may be understood through the interaction between photochemical production, photochemical sink and condensation and advection by the mean meridional circulation. As an example, the decreasing mixing ratio of ethylene (C_2H_4) with altitude in the equatorial stratosphere may be interpreted as advection of enriched air coming from the lower-winter polar stratosphere towards the equator along a partial return branch of the dominant meridional cell.

Figure 4 shows observed and modelled stratospheric latitudinal profiles of acetylene (C_2H_2) and hydrogen cyanide (HCN), as well as vertical profiles at the equator and 80° N. In the Cassini/CIRS latitudinal profiles of stratospheric composition, the summer hemisphere (South) has been investigated at high latitudes (up to roughly 80° S), which was not the case in the Voyager 1/IRIS data, limited to 50° S. In the whole Southern Hemisphere, the observed composition is homogeneous. This is not the case in the modelled composition, as discussed in Crespin *et al.* (2008). In the modelled circulation, as seen in figure 1, the ascending motion goes from roughly 40° S at 60 mbar to the pole at 1 mbar, with a small stratospheric cell located over the summer pole that maintains some descending air over the polar region in the low stratosphere. The air rising in the ascending branch contains smaller abundances of condensable compounds than in other regions, since it comes through the tropopause where condensation occurs. Over the summer pole, the descending air due to this small remaining cell maintains enrichment from spring into summer. The signature of this behaviour is visible in the modelled latitudinal profiles, with a drop at southern mid latitudes, and a remaining enrichment over the South Pole

(figure 4*a*). Since this is not observed, there must be some process missing in the GCM. Even if this secondary cell is not present at the Cassini epoch in the real Titan atmosphere, the ascending motions should still induce a visible drop in the latitudinal profiles. A possible explanation may come from a mixing process, which would erase the latitudinal contrasts in the summer hemisphere, and that is missing in our GCM. Extending the model to three dimensions might be a good test for this problem, since the two-dimensional limitations of our current model may be the reason why such processes could be missing.

The GCM simulations do not fit the observations perfectly well, of course. But the agreement is good enough to demonstrate the role played by advection in the observed features, and therefore confirm that these distributions may be used as a diagnostic for dynamical structures. A significant question still to be addressed concerns the latitudinal and vertical structure of the winter polar vortex, and why the vertical profiles of the observed mixing ratios exhibit a local minimum at approximately 0.1–0.01 mbar for many compounds retrieved at 80° N (Vinatier *et al.* 2007) and 54° N (Vinatier 2007). This minimum is small, but visible, for C_2H_2 in figure 4*b*. These minima cannot be explained with current simulations, and they may be diagnostics of a missing process, though no satisfying hypothesis has been suggested so far.

These variations in the meridional distribution of chemical compounds, induced by dynamical transport, have also a feedback on the temperature structure and dynamics, owing to the radiative role of some compounds. Ethane (C_2H_6), acetylene (C_2H_2) and HCN are radiatively active. The winter polar enhancement of the mixing ratios of these compounds induces a significant additional cooling in the upper stratosphere (above 0.2 mbar), as well as additional heating below 1 mbar (Lebonnois *et al.* 2003). The amplitudes of these effects in this model are -20 and $+7$ K, respectively. Considering the strong impact of the variations of the haze layer on the temperature field, these variations due to composition are only of second order, but should still be taken into account to complete the coupling between composition and dynamics.

5. Tropospheric clouds and dynamics

A first thought at the production of clouds in the atmosphere of Titan indicates two different potential natures for these clouds. They can be produced by motion of air, which may cool for different reasons (adiabatic and radiative cooling in ascending motions or horizontal motions) in the troposphere and they are essentially made of methane. They can also be produced by the cooling of stratospheric air that crosses the lower stratosphere and the tropopause, predominantly at the winter pole, though a similar descent of air is also obtained in the model through the summer polar tropopause. In that case, clouds are made of any photochemical by-products coming from the stratosphere, which are able to condense under these conditions. In models, species that are generally considered are methane (Tokano *et al.* 2001; Mitchell *et al.* 2006; Rannou *et al.* 2006) and ethane because it is the most abundant photochemical by-product and it is representative of the other species (Rannou *et al.* 2006). Figure 5 shows a global view of the cloud layer predicted by our model, compared with the clouds that are reported up to now. Clouds have been observed both using ground-based

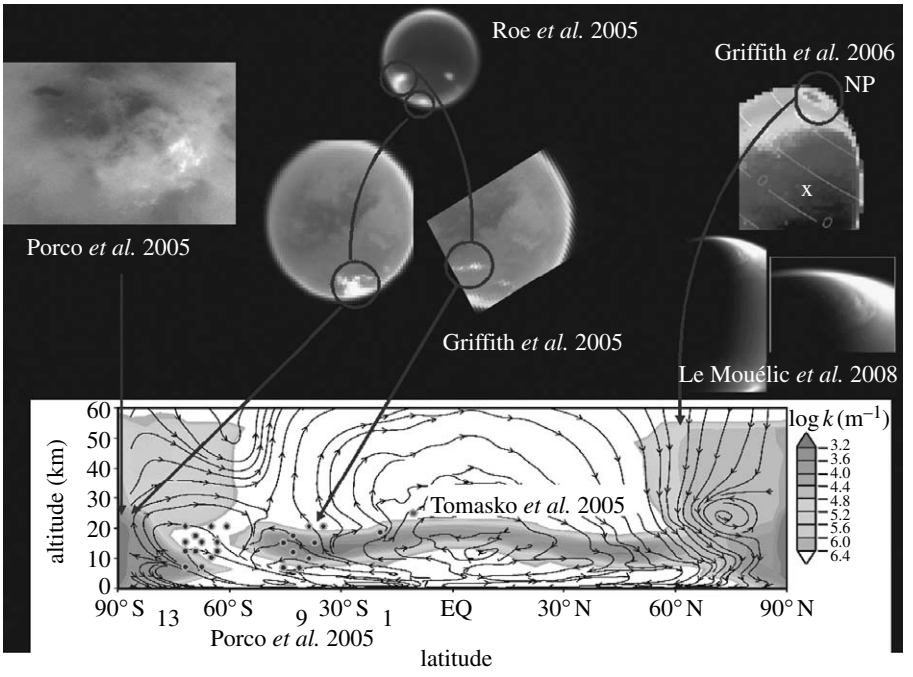

Figure 5. Meridional distribution of cloud extinction at 620 nm, at $L_s \sim 300°$ (from Rannou *et al.* 2006), together with a collection of clouds observations: methane summer polar clouds and southern mid-latitudes clouds (Griffith *et al.* 2005; Porco *et al.* 2005; Roe *et al.* 2005*a*), and ethane winter polar clouds (Griffith *et al.* 2006; Le Mouélic *et al.* 2008). A cloud observed during the Huygens descent is also indicated (Tomasko *et al.* 2005).

telescopes (Brown *et al.* 2002; Roe *et al.* 2005*a*) and with Cassini and Huygens instruments (Griffith *et al.* 2005, 2006; Porco *et al.* 2005; Tomasko *et al.* 2005; Le Mouélic *et al.* 2008). In both cases, these clouds are mainly located at the South Pole and approximately 40° S. As shown in figure 5 (and discussed in more detail in Rannou *et al.* 2006), our model is able to explain the occurrence of these clouds in these regions at this season.

Methane clouds are strongly linked to the circulation. In all models, they appear in the ascending branch of the tropospheric Hadley cell. However, the exact features of cloud cycle and the related precipitations are strongly dependent on the boundary conditions (surface inertia, location of methane source) and the underlying physical processes (cloud microphysics, diffusion processes, thermodynamics, radiative transfer and the detail of dynamics equations). Several differences exist between our model and the models of Tokano and Mitchell; first, we run a two-dimensional axisymmetric version with three-dimensional aspects of the circulation parametrized (interaction between barotropic waves and the mean circulation in the winter jet). In the Tokano model (Tokano *et al.* 2001), circulation is explicitly computed from the equations of meteorology in three dimensions. In the Mitchell model (Mitchell *et al.* 2006), circulation is also treated with a two-dimensional axisymmetric model, but horizontal mixing processes are omitted for simplicity. Another important difference is the way in which cloud microphysics is treated. In our model, we include the physics of cloud microphysics regarding

nucleation, condensation and sedimentation. On the other hand, the Tokano and Mitchell models trigger cloud formation when supersaturation exceeds unity. Methane in excess is instantaneously transported into lower layers. No drop size or cloud opacity can be predicted.

The three models predict clouds or condensation to form in the convergence zone of the Hadley cell. But, this convergence zone is predicted to be fixed very close to the equator (Tokano *et al.* 2001) or to swing from one pole to the other, with various amplitudes and phases, depending on the ground thermal inertia and the thermodynamic feedback due to latent heat exchanges during methane evaporation/condensation (Mitchell *et al.* 2006). Our model predicts an ascending branch of the Hadley cells between 30° and 40° in the summer hemisphere, and descending branches at 60° in both hemispheres. We assume a dry surface (no latent heat due to evaporation, and a thermal inertia of 2000 SI, typical of the Earth continental surfaces), but a methane mixing ratio artificially set to 60 per cent humidity. Below 20 km, we also find a strong horizontal diffusion due to inertial instabilities, which are also predicted by the Tokano model, and probably observed by HASI on Huygens (F. Ferri 2008, personal communication). This zone of horizontal diffusion is important for the cloud and methane cycles; it makes it difficult to accumulate methane between the two tropics since diffusion transports it poleward. This process tends to maintain a constant mixing ratio everywhere, but because the troposphere temperature drops sharply between 30 and 50°, the saturation ratio becomes much larger than one at these latitudes, and methane condenses. This acts as a horizontal cold trap for methane, and it produces a cloudy zone, which is enhanced in the ascending branch of the Hadley cell, at 40° in the summer hemisphere. Neither Tokano *et al.* (2001) nor Mitchell *et al.* (2006) report such a process. For the Tokano *et al.* (2001) model, this is obviously due to a very small latitudinal gradient of temperature. Mitchell *et al.* (2006) essentially give information about the insolation and the precipitation. They neither give information about the temperature field in their model, nor about the place where methane may condense without precipitation. Aside from the cloudy zone at $\pm 40°$, our model also generates small sporadic clouds in the middle troposphere (between 10 and 20 km), anywhere near the equator and between the tropics. This is due to the methane reaching supersaturation while transported upward. These clouds are small and sporadic because they involve a small amount of methane, they are triggered by small fluctuations of temperature and vanish rapidly. Clouds at 40° (in the Southern Hemisphere) have been observed almost simultaneously by Roe *et al.* (2005*a*,*b*) and by Cassini instruments (Griffith *et al.* 2005; Porco *et al.* 2005). The analysis shows that the tops of these clouds are located between 20 and 40 km, and that they are convective. Our model does not account for the convective nature of the clouds, and it predicts their base to be at approximately 10 km. Only the thicker convective clouds can probably be observed from space. Other clouds remain not or hardly observable (Porco *et al.* 2005; Tomasko *et al.* 2005), as, for instance, the numerous clouds between tropics and the cloud at 40° in the winter (Northern) Hemisphere. Further statistical work on cloud coverage will allow us to refine the comparisons and maybe to call into question some of our results. The existence, or the absence, of a specific spot of clouds at 40° N that might be observed with Cassini will be important to better understand the climate in the troposphere.

Poleward to the descending branches of the Hadley cell, we find a regime of slantwise cells that are triggered by the temperature contrast near the pole. In our two-dimensional model, they are associated with thermal instabilities between the (warm) surface at 60° and the cold air at 20 km, at the poles. They correspond to baroclinic waves that we find on the Earth and Mars. Our two-dimensional model cannot predict the real aspect of this circulation, and neither Tokano *et al.* (2001) nor Mitchell *et al.* (2006) mention them in their respective models. However, since baroclinic waves should not be developed on a slowly rotating body such as Titan, the corresponding circulation could be different from that on the Earth or Mars. As any motion of air from a warmer region to a colder region, this cell system is able to produce clouds at both poles, and is thought to be responsible for the south polar cloud system which has been observed for a few years now (e.g. Brown *et al.* 2002; Griffith *et al.* 2005; Porco *et al.* 2005; Hirtzig *et al.* 2006).

Our model also predicts the drop size and lifetime of the clouds (Rannou *et al.* 2006). Methane cloud drop size essentially depends on the amount of methane that is available in excess from the saturation and on the number of nucleation seeds on which methane can condense. The model predicts a methane drop radius of several tens to 100 μm. Owing to the sedimentation speed of such drops the cloud is known to have a short lifetime of several hours. Analysis of photometric observation is also consistent with this prediction (Griffith *et al.* 2005).

By comparison, the ethane clouds are easier to explain, because the circulation producing these clouds is a robust feature, less subject to model-related cautions. The pole-to-pole stratospheric cell is strongly enriched with aerosols and chemical species in its descending branch, near the winter pole. Just above the tropopause (at approx. 50 km) the air becomes cold enough to trigger ethane nucleation and condensation on aerosol particles. Actually, this is also the case for many other species (e.g. C_2H_2, HCN), but only ethane (by far the most abundant) is considered in the model. This produces a vast cloud everywhere between 55° latitude and the pole. Ethane drop radii are calculated to be a few micrometres, making this cloud rather close to a mist or a fog. This cloud is deep, and because the droplets evaporate while the air slowly descends in the troposphere, the base of the cloud depends on the exact temperature field. The cloud reaches the surface and produces precipitation poleward of 80°, whereas it completely vanishes in altitude equator-ward of 80°. It is noteworthy that the evaporation of ethane drops in the polar region is the main source of ethane in the troposphere. This cloud was observed by VIMS (Griffith *et al.* 2006; Le Mouélic *et al.* 2008), and the droplet size was estimated to a few micrometres. No specific spectral feature allows one to determine, with VIMS spectra, the actual composition of this cloud. Only the similarity with the modelled cloud (latitude and altitude range of the cloud, size of the droplets) enables one to surmise that this cloud is probably made of ethane. Our model also predicts a mixing ratio of ethane in the troposphere larger than the tropopause cold trap, i.e. the mixing ratio corresponding to ethane vapour pressure at the tropopause. This is due to transport of liquid ethane droplets through the cold trap in the winter polar region, followed by cloud evaporation in the troposphere. The amount of ethane transported this way yields a tropospheric mixing ratio of approximately 2.5×10^{-6}.

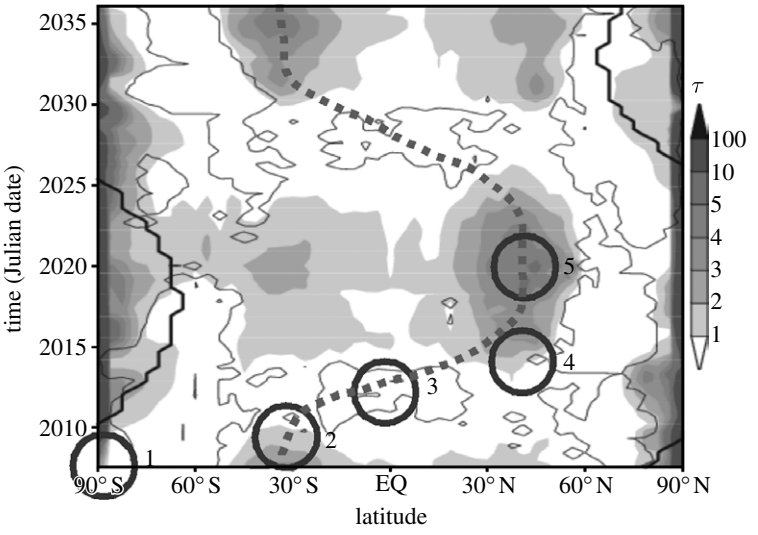

Figure 6. Latitudinal and seasonal evolution of the cloud opacity at 2 μm above 10 km altitude, for 1 Titan year from 2006 (adapted from Rannou *et al.* 2006). The dashed line indicates the subsolar latitude, and the circles show five notable features in the cloud behaviour predicted for the next 15 years (see text).

6. Tropospheric clouds: weather forecast

Up to now, we have essentially discussed the tropospheric clouds at Cassini and Huygens time, and slightly before. Obviously, the main reason is that the first image of Titan cloud is very recent (Brown *et al.* 2002). However, our model predicts cloud distribution for the complete Titan annual cycle. We can thus already foresee several salient features that are predicted to happen in the next 15 years. Obviously, whether or not these features will appear will tell a lot about the atmospheric circulation, and will also be constraining our model.

Figure 6 gives five key points of the cloud cover. First, we predict that the South Pole cloud disappears for several months (up to approx. 2 years, between 2006 and 2008) before the equinox. This is due to a change in circulation in the lowermost layer, driven by the change of insolation at that time. The second event is the gradual disappearance of the recurrent clouds at 40° S, which could be observed as early as 2007, but will be obvious in 2008 or 2009. The third key point is the absence of large clouds near the equator or at mid-latitudes during the equinox transition. That does not exclude the existence of small clouds, similar to the discrete clouds already reported by Porco *et al.* (2005). The fourth feature is the presence of clouds at 40° N which should gradually appear near or after 2015. It is probable that the first occurrence of these clouds will be hard to detect, especially with telescope observations, but the maximum in occurrence and opacity will be reached in 2020. The 2020 date for this cloud system will be equivalent to the maximum for the 40° S cloud in 2005. However, it is noteworthy that Titan's annual cycle is not exactly symmetric, due to its orbit eccentricity. Thus, the model predicts that the cloud system at 40° N in 2020 should be significantly less active that its counterpart at 40° S in 2005.

Except for the interruption before equinoxes, polar methane clouds seem to be a permanent feature. The ethane cloud does not appear in the prediction map since it represents a small opacity compared to methane cloud opacity. It is produced by the descending branch of the stratospheric circulation. Then, it lasts more than 12 years, starts and grows in the autumn polar region after the autumn equinox. It reaches a maximum just before the spring equinox, and then gradually vanishes afterwards. The model predicts that it does not completely disappear, although its maintenance depends on the opposite cell at the summer pole in our model, which may be a model-dependent feature. The ethane cloud has not been observed by Cassini, through the haze, in the South Polar region (summer time). That should give, after analysis, an upper limit for its opacity.

7. Perspectives

Physically based global climate models, developed for decades to study the climate of the Earth, have proven to be relevant and useful tools for other planetary atmospheres. Results obtained for Titan have led to a self-consistent picture covering many of the observed atmospheric features, and highlight the importance of couplings between atmospheric dynamics, haze and composition.

However, our GCM has reached its limits: its two-dimensional characteristic, related to computational time, and its vertical extension, related to radiative transfer limitations. Going beyond these limitations is an ongoing project, and is necessary given recent studies that are pointing towards processes that are not yet included, but may play a significant role in Titan's climatic system.

Using a three-dimensional GCM focused on tropospheric studies, Tokano & Neubauer (2002) show that the gravitational tides induced by Titan's orbit around Saturn in the atmosphere of Titan may have a significant impact on the circulation and temperature structure of the troposphere. Including this process in our GCM requires an extension to a three-dimensional grid. The effect of this process on the tropospheric clouds' distribution needs to be fully assessed. Indeed, this distribution has been observed to be non-axisymmetric, with a preferential occurrence of clouds around zero longitude, facing Saturn (Roe *et al.* 2005*b*). It will also be necessary in this context to explore the possible impact of the diurnal cycle (not included in this two-dimensional geometry), and of the topography (some coverage is now coming from the Cassini Radar, e.g. Stofan *et al.* (2006) and Lunine *et al.* (2008)) on the circulation, and on tropospheric cloud formation.

The role of processes coupling the upper and lower regions of Titan's atmosphere, through the mesosphere (300–600 km altitude region, approx.), needs also to be fully assessed. This region has not been extensively observed, but there are hints that it may play a significant role in Titan's climate, through its controls over the haze layers' distribution. The structures of the upper haze layers in winter polar regions have been observed to be more complex than expected (Porco *et al.* (2005), as well as many Casini/ISS images available at http://photojournal.jpl.nasa.gov/catalogue), and the mesopheric dynamics should certainly play a role there. The production of the haze precursors has recently been linked to ionospheric photochemistry, via the observation of heavy positive and negative ions with Cassini INMS and CAPS instruments (Waite *et al.* 2005).

A recent study of the photochemical cycle of benzene in the upper atmosphere, based on INMS data, also points in the same direction (Vuitton *et al.* 2008). This may give some hints to find a possible explanation to the apparent variations of the altitude of the detached haze layer, observed between the Voyager mission and the Cassini mission. In 1980, this detached layer was observed to be located at approximately 350 km altitude (Rages & Pollack 1983). Today, though many distinct haze layers are visible in the ISS/Cassini images, the intensity (I/F) profiles indicate that the dominant detached haze layer is now located as high as 510 km (Porco *et al.* 2005). If the detached haze layers seen at these two different epochs are indeed correlated, this yields an increase in altitude of roughly 50 per cent though the difference in season is minor, which remains to be understood. Mesospheric photochemical processes and dynamics are therefore certainly strongly coupled to the haze distribution that has a dominant role in the thermal and dynamical structure of Titan's lower atmosphere.

Several atmospheric features remain to be interpreted, as diagnosed by the observed compounds' distributions. The extension of the winter polar vortex remains to be fully constrained by Cassini/CIRS limb observations. Potential processes could be taking place in the high stratosphere of the winter hemisphere, that may explain the observed minima in the molecules abundances, but they remain to be understood. Also, dynamics and mixing processes in the summer stratosphere should be more extensively studied. These discrepancies will need to be addressed in future evolutions of Titan's atmospheric global climate models, especially using full three-dimensional versions of such coupled models.

References

Achterberg, R. K., Conrath, B. J., Gierasch, P. J., Flasar, F. M. & Nixon, C. A. 2008 Titan's middle-atmospheric temperatures and dynamics observed by the Cassini composite infrared spectrometer. *Icarus* **194**, 263–277. (doi:10.1016/j.icarus.2007.09.029)

Bézard, B., Coustenis, A. & McKay, C. P. 1995 Titan's stratospheric temperature asymmetry: a radiative origin? *Icarus* **113**, 267–276. (doi:10.1006/icar.1995.1023)

Bird, M. K. *et al.* 2005 The vertical profile of winds on Titan. *Nature* **438**, 1–3. (doi:10.1038/nature04060)

Brown, M. E., Bouchez, A. H. & Griffith, C. A. 2002 Direct detection of variable tropospheric clouds near Titan's south pole. *Nature* **420**, 795–797. (doi:10.1038/nature01302)

Cabane, M., Chassefière, E. & Israel, G. 1992 Formation and growth of photochemical aerosols in Titan's atmosphere. *Icarus* **96**, 176–189. (doi:10.1016/0019-1035(92)90071-E)

Coustenis, A. & Bézard, B. 1995 Titan's atmosphere from Voyager infrared observations. IV. Latitudinal variations of temperature and composition. *Icarus* **115**, 126–140. (doi:10.1006/icar.1995.1084)

Coustenis, A. *et al.* 2007 The composition of Titan's stratosphere from Cassini/CIRS mid-infrared spectra. *Icarus* **189**, 35–62. (doi:10.1016/j.icarus.2006.12.022)

Crespin, A., Lebonnois, S., Vinatier, S., Bézard, B., Coustenis, A., Teanby, N. A., Achterberg, R. K., Rannou, P. & Hourdin, F. 2008 Diagnostics of Titan's stratospheric dynamics using Cassini/CIRS data and the IPSL general circulation model. *Icarus* **197**, 556–571. (doi:10.1016/j.icarus.2008.05.010)

Dire, J. R. 2000 Seasonal photochemical and meridional transport model for the stratosphere of Titan. *Icarus* **145**, 428–444. (doi:10.1006/icar.2000.6342)

Flasar, F. M. *et al.* 2005 Titan's atmospheric temperatures, winds, and composition. *Science* **308**, 975–978. (doi:10.1126/science.1111150)

Gierasch, P. 1975 Meridional circulation and the maintenance of the Venus atmospheric rotation. *J. Atmos. Sci.* **32**, 1038–1044. (doi:10.1175/1520-0469(1975)032<1038:MCATMO>2.0.CO;2)

Griffith, C. A. *et al.* 2005 The evolution of Titan's mid-latitude clouds. *Science* **310**, 474–477. (doi:10.1126/science.1117702)

Griffith, C. A. *et al.* 2006 Evidence for a polar ethane cloud on Titan. *Science* **313**, 1620–1622. (doi:10.1126/science.1128245)

Hirtzig, M. *et al.* 2006 Monitoring atmospheric phenomena on Titan. *Astron. Astrophys.* **456**, 761–774. (doi:10.1051/0004-6361:20053381)

Hourdin, F., Talagrand, O., Sadourny, R., Courtin, R., Gautier, D. & McKay, C. P. 1995 Numerical simulation of the general circulation of the atmosphere of Titan. *Icarus* **117**, 358–374. (doi:10.1006/icar.1995.1162)

Hourdin, F., Lebonnois, S., Luz, D. & Rannou, P. 2004 Titan's stratospheric composition driven by condensation and dynamics. *J. Geophys. Res.* **109**, E12005. (doi:10.1029/2004JE002282)

Hubbard, W. B. *et al.* 1993 The occultation of 28 Sgr by Titan. *Astron. Astrophys.* **269**, 541–563.

Hutzell, W. T., McKay, C. P., Toon, O. B. & Hourdin, F. 1996 Simulations of Titan's brightness by a two-dimensional haze model. *Icarus* **119**, 112–129. (doi:10.1006/icar.1996.0005)

Lebonnois, S. 2000 Circulation générale et photochimie dans l'atmosphère de Titan. PhD thesis, Université Paul Sabatier, Toulouse.

Lebonnois, S. & Toublanc, D. 1999 Actinic fluxes in Titan's atmosphere, from one to three dimensions: application to high-latitude composition. *J. Geophys. Res.* **104**, 22 025–22 034. (doi:10.1029/1999JE001056)

Lebonnois, S., Toublanc, D., Hourdin, F. & Rannou, P. 2001 Seasonal variations in Titan's atmospheric composition. *Icarus* **152**, 384–406. (doi:10.1006/icar.2001.6632)

Lebonnois, S., Hourdin, F., Rannou, P., Luz, D. & Toublanc, D. 2003 Impact of the seasonal variations of ethane and acetylene distributions on the temperature field of Titan's stratosphere. *Icarus* **163**, 164–174. (doi:10.1016/S0019-1035(03)00074-5)

Le Mouélic, S. *et al.* 2008 Imaging of the North Polar Cloud on Titan by the VIMS imaging spectrometer onboard Cassini. *39th Lunar and Planetary Science Conf., Houston, 10–14 March.*

Lunine, J. I. *et al.* 2008 Titan's diverse landscapes as evidenced by Cassini RADAR's third and fourth looks at Titan. *Icarus* **195**, 415–433. (doi:10.1016/j.icarus.2007.12.022)

Luz, D. & Hourdin, F. 2003 Latitudinal transport by barotropic waves in Titan's stratosphere. I. General properties from a horizontal shallow-water model. *Icarus* **166**, 328–342. (doi:10.1016/j.icarus.2003.08.015)

Luz, D., Hourdin, F., Rannou, P. & Lebonnois, S. 2003 Latitudinal transport by barotropic waves in Titan's stratosphere. II. Results from a coupled dynamics–microphysics–photochemistry GCM. *Icarus* **166**, 343–358. (doi:10.1016/S0019-1035(03)00263-X)

Luz, D. *et al.* 2005 Characterization of zonal winds in the stratosphere of Titan with UVES. *Icarus* **179**, 497–510. (doi:10.1016/j.icarus.2005.07.021)

Mitchell, J. L., Pierrehumbert, R. T., Frierson, M. W. & Caballero, R. 2006 The dynamics behind Titan's methane cloud. *Proc. Natl Acad. Sci. USA* **103**, 18 421–18 426. (doi:10.1073/Pnas.0605074103)

Moreno, R., Marten, A. & Hidayat, T. 2005 Interferometric measurements of zonal winds on Titan. *Astron. Astrophys.* **437**, 319–328. (doi:10.1051/0004-6361:20042117)

Niemann, H. B. *et al.* 2005 The abundances of constituents of Titan's atmosphere from the GCMS instrument on the Huygens probe. *Nature* **438**, 1–6. (doi:10.1038/nature04122)

Porco, C. C. *et al.* 2005 Imaging of Titan from the CASSINI spacecraft. *Nature* **434**, 159–168. (doi:10.1038/nature03436)

Rages, K. & Pollack, J. B. 1983 Vertical distribution of scattering hazes in Titan's upper atmosphere. *Icarus* **55**, 50–62. (doi:10.1016/0019-1035(83)90049-0)

Rannou, P., Cabane, M., Chassefière, E., Botet, R., McKay, C. P. & Courtin, R. 1995 Titan's geometric albedo: role of the fractal structure of the aerosols. *Icarus* **118**, 355–372. (doi:10.1006/icar.1995.1196)

Rannou, P., Hourdin, F. & McKay, C. P. 2002 A wind origin for Titan's haze structure. *Nature* **418**, 853–856. (doi:10.1038/nature00961)

Rannou, P., Hourdin, F., McKay, C. P. & Luz, D. 2004 A coupled dynamics–microphysics model of Titan's atmosphere. *Icarus* **170**, 443–462. (doi:10.1016/j.icarus.2004.03.007)

Rannou, P., Lebonnois, S., Hourdin, F. & Luz, D. 2005 Titan atmosphere database. *Adv. Space Res.* **36**, 2194–2198. (doi:10.1016/j.asr.2005.09.041)

Rannou, P., Montmessin, F., Hourdin, F. & Lebonnois, S. 2006 The latitudinal distribution of clouds on Titan. *Science* **311**, 201–205. (doi:10.1126/science.311.5758.141c)

Roe, H. G., de Pater, I., Macintosh, B. A., Gibbard, S. G., Max, C. E. & McKay, C. P. 2002 Titan's atmosphere in late southern spring observed with adaptive optics on the W.M. Keck II 10-meter telescope. *Icarus* **157**, 254–258. (doi:10.1006/icar.2002.6831)

Roe, H. G., Bouchez, A. H., Trujillo, C. A., Schaller, E. L. & Brown, M. E. 2005*a* Discovery of temperate latitude clouds on Titan. *Astrophys. J. Lett.* **618**, L49–L52. (doi:10.1086/427499)

Roe, H. G., Brown, M. E., Schaller, E. L., Bouchez, A. H. & Trujillo, C. A. 2005*b* Geographic control of Titan's mid-latitude clouds. *Science* **310**, 477–479. (doi:10.1126/science.1116760)

Rossow, W. B. & Williams, G. P. 1979 Large-scale motion in the Venus stratosphere. *J. Atmos. Sci.* **36**, 377–389. (doi:10.1175/1520-0469(1979)036<0377:LSMITV>2.0.CO;2)

Sicardy, B. *et al.* 2006 The two Titan stellar occultations of 14 November 2003. *J. Geophys. Res.* **111**, E11S91. (doi:10.1029/2005JE002624)

Smith, G. R., Strobel, D. F., Broadfoot, A. L., Sandel, B., Shemansky, D. E. & Holberg, J. B. 1982 Titan's upper atmosphere: composition and temperature from the EUV solar occultation results. *J. Geophys. Res.* **87**, 1351–1359. (doi:10.1029/JA087iA03p01351)

Stofan, E. R. *et al.* 2006 Mapping of Titan: results from the first Titan Radar passes. *Icarus* **185**, 443–456. (doi:10.1016/j.icarus.2006.07.015)

Teanby, N. A. *et al.* 2006 Latitudinal variations of HCN, HC_3N and C_2N_2 in Titan's stratosphere derived from Cassini CIRS data. *Icarus* **181**, 243–255. (doi:10.1016/j.icarus.2005.11.008)

Teanby, N. A. *et al.* 2007 Vertical profiles of HCN, HC_3N and C_2H_2 in Titan's atmosphere derived from Cassini/CIRS data. *Icarus* **186**, 364–384. (doi:10.1016/j.icarus.2006.09.024)

Teanby, N. A. *et al.* 2008 Global and temporal variations in hydrocarbons and nitriles in Titan's stratosphere for northern winter observed by Cassini/CIRS. *Icarus* **193**, 595–611. (doi:10.1016/j.icarus.2007.08.017)

Tokano, T. & Neubauer, F. M. 2002 Tidal winds on Titan caused by Saturn. *Icarus* **158**, 499–515. (doi:10.1006/icar.2002.6883)

Tokano, T., Neubauer, F. M., Laube, M. & McKay, C. P. 2001 Three-dimensional modeling of the tropospheric methane cycle on Titan. *Icarus* **153**, 130–147. (doi:10.1006/icar.2001.6659)

Tomasko, M. G. *et al.* 2005 Rain, winds and haze during the Huygens probe's descent to Titan's surface. *Nature* **438**, 1–14. (doi:10.1038/nature04126)

Toon, O. B., McKay, C. P., Griffith, C. A. & Turco, R. P. 1992 A physical model of Titan's aerosols. *Icarus* **95**, 24–53. (doi:10.1016/0019-1035(92)90188-D)

Vinatier, S. 2007 Analyse des spectres infrarouge thermiques de l'atmosphère de Titan enregistrés par l'instrument CIRS à bord de Cassini. PhD thesis, Université Paris VII.

Vinatier, S. *et al.* 2007 Vertical abundance profiles of hydrocarbons in Titan's atmosphere at 15° S and 80° N retrieved from Cassini/CIRS spectra. *Icarus* **188**, 120–138. (doi:10.1016/j.icarus.2006.10.031)

Vuitton, V., Yelle, R. V. & Cui, J. 2008 Formation and distribution of benzene on Titan. *J. Geophys. Res.* **113**, E05007. (doi:10.1029/2007JE002997)

Waite Jr, J. H. *et al.* 2005 Ion neutral mass spectrometer results from the first flyby of Titan. *Science* **308**, 982–986. (doi:10.1126/science.1110652)

Yung, Y. L. 1987 An update of nitrile photochemistry on Titan. *Icarus* **72**, 468–472. (doi:10.1016/0019-1035(87)90186-2)